

Article

# Raised Pedestrian Crossings: Analysis of Their Characteristics on a Road Network and Geometric Sizing Proposal

Giuseppe Loprencipe , Laura Moretti \* , Antonio Pantuso  and Eligio Banfi

Department of Civil, Constructional and Environmental Engineering, Sapienza University of Rome,  
Via Eudossiana 18, 00184 Rome, Italy

\* Correspondence: laura.moretti@uniroma1.it; Tel.: +39-064-458-5114

Received: 15 May 2019; Accepted: 12 July 2019; Published: 16 July 2019



**Abstract:** In urban areas traffic-calming strategies and pedestrian friendly measures are often adopted to reduce the adverse impacts of motor vehicles on vulnerable users. This study surveyed 24 raised pedestrian crossings (RPCs) to examine their geometrical and functional characteristics. Geometric characteristics, location, administrative and effective vehicle speed, and the whole-body vibration acceleration induced to vehicle occupants while they are passing over, were considered. In addition to the analysis of the field data, geometrical and functional criteria to design RPCs were carried out. Particularly, two design approaches have been considered. In the first one, RPC provides a designated route across a carriageway raised to the same level, or close to the same level, as the sidewalks that provide access to the pedestrian crossing. In such condition, an RPC is not a traffic-calming device and its design should satisfy geometrical and comfort criteria for designing roads. The results from the surveys demonstrated that less than 10% of RPCs guarantee ride comfort. According to the second design approach, an RPC acts both as a marked pedestrian feature and as a traffic-calming device (i.e., it is trapezoidal in shape with sharp edges). The analysis of the vertical accelerations on vehicle occupants reveal that more than 90% of the surveyed RPCs comply with geometrical and dynamic criteria for speed tables. Extreme variations concerning the observed geometrical characteristics of RPCs and the modelled dynamic performances have been observed: It results in noneffective treatments. Therefore, the results of this study would contribute to providing geometric best practices for overcoming the regulation gap in this subject, and designing RPCs according to international standards.

**Keywords:** raised pedestrian crossings; speed tables; speed control undulations; pedestrian infrastructure; traffic calming; pedestrian crossing

---

## 1. Introduction

Pedestrian safety is one of the main concerns in modern society. Each year, more than 270,000 pedestrians lose their lives on the world's roads, and they constitute two thirds of all road traffic deaths [1]. Despite the reduction of fatalities in European countries in recent years, an increase in fatalities in urban areas has been recorded [2–5]. As a consequence, traffic engineers and urban planners have increased their focus on vulnerable road users [6–10]. Accordingly, traffic safety countermeasures have been developed in urban areas to improve the safety of pedestrians and cyclists [11,12]. The most important factor in pedestrian injuries from vehicle collisions is the impact speed [13,14]. Therefore, the most frequently adopted countermeasures aim to reduce vehicle speed, to regulate traffic flow within a road section, and to increase drivers' attention. These aspects are important in the actual panorama where the concept of urban walkability is being introduced and the attention paid to

pedestrian infrastructures is increasing [15,16]. Over the years, different systems have been adopted to reduce the risk of vehicle–pedestrian collisions, especially in urban areas. Speed control undulations (SCUs) are traffic-calming units that aim to increase pedestrian safety, as well as reduce noise and pollution from traffic in residential areas.

Undulations are usually installed on residential, local, or collector roads; at any rate, these urban roads should not have buses, emergency traffic or, in general, heavy traffic, and should have an administrative speed limit of 20 or 30 km/h [5,17]. A warning sign with an adequate speed limit sign should be installed before an undulation [1,18]. When 15% of traffic exceeds the speed limit by 8–16 km/h the enforcement band is not effective [19], and the road manager could evaluate the installation of SCUs and/or other traffic-calming systems.

Raised pedestrian crossings (RPCs) are used in urban areas to increase the walkability of neighborhoods [20] and to reduce the probability of pedestrian injuries and fatalities after a crash, either within specific traffic-calming programs, or more generally within Sustainable Urban Mobility Plans, with increased road safety being one of the main priorities in these regulatory tools [21]. The vertical profile of RPCs should comply with dynamic and geometric criteria adopted to designs as a vertical road alignment. In many roads, RPCs are used as SCUs, but this use is only a ploy of the designer or road manager to install a SCU where it is not admitted. In fact, RPCs, unlike SCUs, have no application limits related to road type and are widely used at every type of intersection, and where different traffic functions coexist. A typical example is to locate more bus stops close to raised intersections to enable passengers to minimize travel times and distances while changing lines from one stop to another [22], and thus walk freely across the raised area. RPCs could be more suitable also to mitigate the severity of risks associated with powered two-wheelers (PTWs) when approaching intersections due to fast riding habits, although studies on PTW accidents [23,24] stress the need to advance knowledge in this field.

A broad range of traffic-calming units have been installed in urban areas recently. Vehicle restrictions, warning signs, gateways, speed tables, median islands, channelization islands, speed humps, rumble strips, mini-circles, roundabouts, special pavements and markings, central hatching, warning signs, radar clocked traffic speeds displayed to drivers, lane narrowing, horizontal shifts, and speed control units such as raised pedestrian crossings, speed bumps, or speed humps [5,25,26] are the most frequently adopted systems. On the other hand, RPCs encourage drivers to yield to pedestrians: Signed and marked facilities provide a continuous route for pedestrians at the same level as the sidewalk. Therefore, pedestrians do not encounter curb ramps and vehicles should slow down their operating speed, thus reducing the risk of injury to pedestrians [6]. However, local authorities are not using in an appropriate manner both SCUs [14] and RPCs, and there is a lack of regulations on traffic control design [27]. Likewise, exhaustive and long-term studies on the implementation of both in areas with powered two-wheelers (PTWs) are still lagging behind, in spite of the need for such knowledge for fine-tuning the economic assessment of risks and maintenance programs associated with this mode, which although reliable, do not consider effects of traffic calming on PTWs [23,24].

In the literature, several studies about the effect of geometric design criteria of SCUs (i.e., slope, height, and length) and their effectiveness in reducing vehicle speed are available [14,28–32]. SCU studies show that drivers approaching a hump reduce vehicle speed in order to mitigate the discomfort caused by the vertical accelerations in the vehicle overpassing the SCU. On the other hand, other studies focused on the discomfort of vehicle occupants moving over the SCU by studying the effects of the vehicle occupants' whole-body vibrations on human health [33–35], using a quarter car [36], half car [28,37], or full car model [38] to simulate the vehicle moving over SCUs.

This paper considers an experimental campaign performed in an Italian urban road network where RPCs are located. The results of the campaign allowed for the analysis of the geometrical and functional performances of RPCs in terms of the comfort and safety of the vehicle users. Different values of vehicle speed and profiles of RPCs (i.e., longitudinal slope of access and exit ramps) have been considered to compare the surveyed RPCs to the theoretical results from the implementation of

two Italian standards for designing roads and speed tables. The results of the study could be adopted to properly design RPCs or speed tables where pedestrian crossings are planned.

## 2. Methods

In this study, the authors proposed a geometrical and functional analysis of raised pedestrian crossings considering their geometry, layout, and traffic. The study is composed of an in situ survey and a post-processing analysis.

Table 1 represents the survey sheet used during fieldwork to check the main attributes of each RPC.

**Table 1.** Raised pedestrian crossing (RPC) survey sheet.

Branch Name	Section ID	GPS Location
Road Name ID	RPC ID	Latitude and Longitude in WGS84 Projection
Street View® WebLink		
Surveyed By/Date:	Inspector Name	Date
<b>Visual survey report</b>		
Item n.	Survey parameters	Attribute:
1	Road Type	Primary Road; Secondary Road; Residential Area Road
2	Administrative speed limit	50 km/h; 40 km/h; 30 km/h
3	Measured speed	Value
4	<b>Pavement Condition Assessment *</b>	
4.1	20 m before RPC Facility	Adequate; Medium; Unsatisfactory
4.2	Before RPC Facility	Adequate; Medium; Unsatisfactory
4.3	RPC ramp before speed table	Adequate; Medium; Unsatisfactory
4.4	RPC speed table	Adequate; Medium; Unsatisfactory
4.4	RPC ramp after speed table	Adequate; Medium; Unsatisfactory
4.6	After RPC Facility	Adequate; Medium; Unsatisfactory
4.7	20 m after RPC Facility	Adequate; Medium; Unsatisfactory
5	<b>RPC materials</b>	
5.1	RPC ramps materials	Asphalt Concrete; Cement Concrete; Natural Stone; Interlocking pavements; Plastic materials
5.2	RPC speed table materials	Asphalt Concrete; Cement Concrete; Natural Stone; Interlocking pavements; Plastic materials
6	<b>Countermeasures for speed control</b>	
6.1	Horizontal Markings	None; Strips; Reflective Strips; Lane Narrowing Marking
6.2	Vertical signs	None; RPC Warning; RPC Warning Reflective
6.3	Sight obstacles	None; Trash bin; Parking Spots; Bus Stop
6.4	Lighting	None; Illuminated RPC

\* Rating method according to [39].

In the top part of the sheet, the road identification data are recorded: Branch name, section ID, GPS coordinates reference, and Google Street View® weblink; geolocation data are useful during the back-analysis process. In the bottom part of the sheet, the recorded road parameters are: Road type;

administrative speed limit of the road; value of the measured speed; pavement condition assessment of the RPC area in order to identify and report localized distresses such as depression produced by the vehicle dynamic loading while passing along the RPC; RPC materials; and presence of additional countermeasures for speed control (i.e., horizontal marking, vertical marking, sight obstacles, and illumination). For each of these parameters, road attributes are coded as numeric inputs according to Table 1. To measure the vehicle speed, the authors used a self-made device (Figure 1a) composed of an electronics platform able to read input light on a sensor (Figure 1b), and two infrared sensors, a transmitter, and a receiver (Figure 1c) which are fixed 1 m apart and are in a circuit. The self-made device for vehicle speed measurement was assembled using Arduino electronic components and a longitudinal iron bar. The instrument calculates the speed of passing vehicles based on interrupting the connection between the two IR. When a vehicle passes, the first IR transmits a signal to the electronic platform, which starts counting the time until the second IR transmits a new signal. The IRs scope ranges between 1 and 5.5 m: It allows for measuring the vehicle speed of one lane of traffic. Therefore, it can be used on a 1-lane road, or on a 2-way road with one lane per way. The device was validated with the GPS vehicle speed in the range of speed from 20 km/h to 80 km/h, finding not more than  $\pm 10\%$  difference.

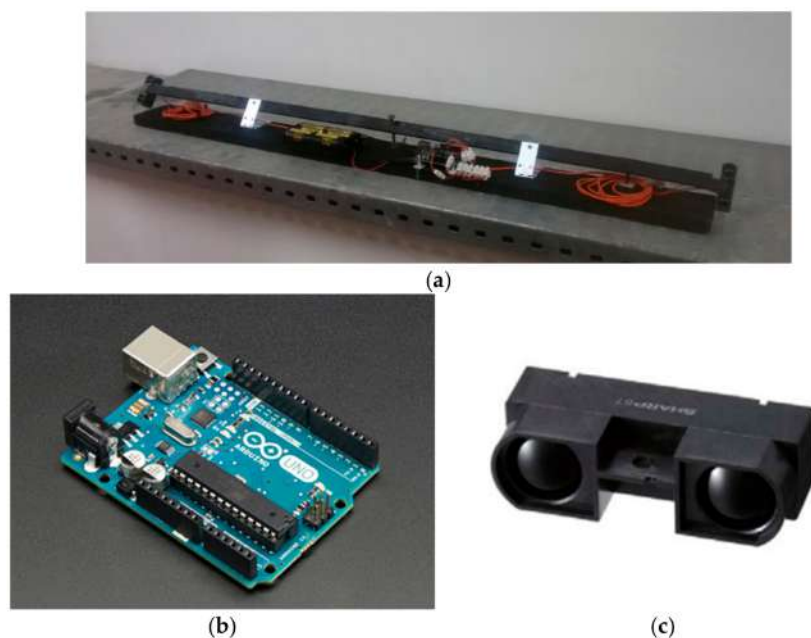


**Figure 1.** Speed measuring instrument: (a) Self-made device; (b) sensor; (c) two infrared sensors.

All speed measures were collected under low-volume conditions (i.e., free-flow conditions). According to [40], it occurs when drivers are free to travel at their desired speed and are not constrained by the presence of other vehicles or downstream traffic control devices. For each RPC, all the measurements occurred during four 15 min intervals within a working day. The device for measuring speed was installed at the half speed table point.

The geometrical characteristics of each RPC were measured according to [41], using the hand-held Dipstick device [42]. These measurements allowed for the calculation of the inclination of the ramps ( $i_a$  for approach ramp,  $i_e$  for exit ramp), the medium height ( $h_m$ ), the length of the approach ramp ( $L_A$ ), the length of exit ramp ( $L_E$ ), the length of flat top ( $L_f$ ), and the total length of the RPC ( $L_T$ ) (Figure 2). Primary data about geometry of the surveyed RPCs are in the Supplementary Materials.

Given the longitudinal profiles, the whole-body vibrations (WBV) experienced by vehicle occupants were estimated by simulating the passage of the full car model on each surveyed RPC. An 8-degrees-of-freedom (dof) vehicle model full car simulated the passage at 4 speed values [38,43]: 20 km/h, 30 km/h, 40 km/h, and 50 km/h.

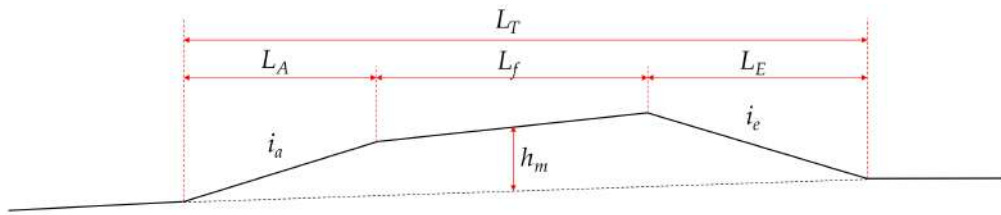


Figure 2. Geometrical characterization of an raised pedestrian crossing (RPC).

The 8-dof vehicle model was developed by Cantisani and Loprencipe [38], and was calibrated in order to represent the behavior of a passenger car using the ISO 2631 approach [44], calculating the vertical frequency-weighted accelerations ( $a_{wz}$ ) as described in the same standard.

First, considering each of the longitudinal profiles of surveyed RPC, the vertical accelerations  $a_z$  in the time domain were calculated at the 4 speeds considered. After, the mean square accelerations (RMS) of the root were calculated through the evaluation of the power spectral density, in correspondence with all 23 bands of a third of an octave, covering the frequency interval of interest for the human response to vibrations (between 0.5–80 Hz), as specified by the technical standards in use.

So, the RMS accelerations (calculated of each profile and of each speed) were used to calculate the vertical weighted RMS acceleration ( $a_{wz}$ ) using Equation (1):

$$a_{wz} = \sqrt{\sum_{i=1}^{23} (W_{k,i} \cdot a_{iz}^{RMS})^2} \tag{1}$$

where  $W_{k,i}$  are the frequency weightings in one-third octave bands for seated position, provided by the standards, and  $a_{iz}$  is the vertical RMS acceleration for the  $i$ -th one-third octave band.

This method (Figure 3) allowed the evaluation of the vertical accelerations in order to analyze the comfort of car passengers [39,45,46].

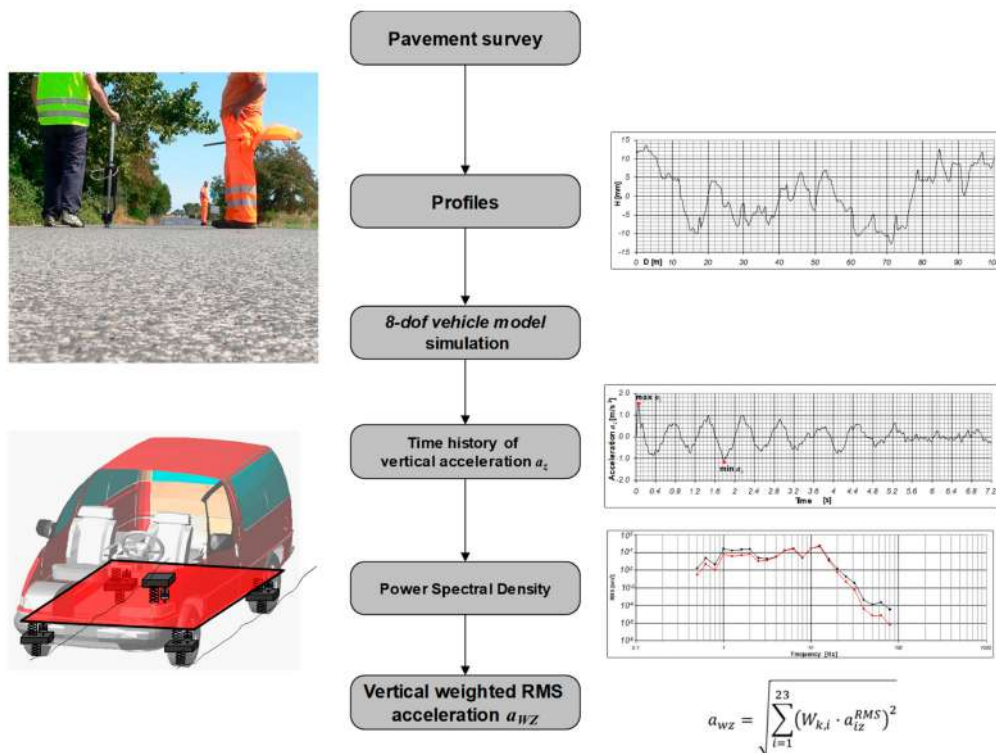


Figure 3. Flow chart of the method used for the evaluation of the vertical weighted mean square accelerations (RMS) of the root  $a_{wz}$ .

### 3. Results

This study is based on the results of surveys carried out on RPCs in Italian urban areas (Figure 4).



Figure 4. Example of RPC.

Twenty four two-way roads with RPCs were considered (each observed RPC is named as “site N”, where N ranges between 1 and 24; when two directions have been measured, the letters “a” and “b” are added after the ID “site N”). The campaign consisted of visual surveys, measurements of the RPC’s geometrical characteristics, and measurement of the effective speed of vehicles passing along the RPC.

Table 2 summarizes the results of the visual surveys. It highlights that pavement depressions before RPCs and localized damages on RPCs are 21% and 34% of the survey sample, respectively. For all the surveyed RPCs vertical signs were present, while only 17% had horizontal markings on the RPC; 12% of sites did not have horizontal markings after ramps.

Table 2. Overview of visual survey results.

Attribute	Number of RPCs (% of RPCs)
Depressions before/after RPC	5 (21%)
Localized damages	8 (34%)
Horizontal markings on RPC ramps	21 (88%)
Horizontal markings before RPC	4 (17%)
Vertical signs	24 (100%)

Figure 5 shows the most frequently observed distresses and damages on the road pavement: Depressions on the access ramp (Figure 5a) or after the exit ramp (Figure 5b), and grooves on the pedestrian crossing surface (Figure 5c) or after (Figure 5d) the RPC, which indicate vehicle–pavement contact.

Figure 6 shows the RPC longitudinal profile obtained from Dipstick for two surveyed RPCs (i.e., site 1b and site 17 in Figure 6a,b, respectively) where the administrative speed limit is 40 km/h. Both curves describe the pavement profile along the centerline of each RPC.

During the surveys, the self-made device measured the effective speed of vehicles through each RPC: Figure 7a,c represent the relative speed distributions measured at the half speed table points of site 1b and site 17 (i.e., profiles in Figure 6a,b) respectively. Although the speed distribution is discrete, the Gaussian curve can fit the experimental values: Figure 7b,d refer to the relative speed distributions in Figure 6a,c, respectively.

The results in Figure 7 highlight that about 14% and 7% of drivers passing through site 1b and 17, respectively, do not respect the speed limit (i.e., 40 km/h).

Given the longitudinal profiles in Figure 6, Figure 8 shows the trend of the calculated values of  $a_z$  that could be experienced on board at four speed values (i.e., 20 km/h, 30 km/h, 40 km/h, and 50 km/h). These values are even more than the administrative speed limit set for site 1b and 17, but they reflect the surveyed speed values. In regards to site 1b, Figure 8a,b represent the values of  $a_z$  and the elevation curve, respectively; Figure 8c,d refer to the values of  $a_z$  and the elevation curve of site 17.



**Figure 5.** Example of surveyed distresses: (a) Depression on the access ramp; (b) depression after the exit ramp; (c) grooves on the pedestrian crossing surface; (d) grooves after the pedestrian crossing surface.

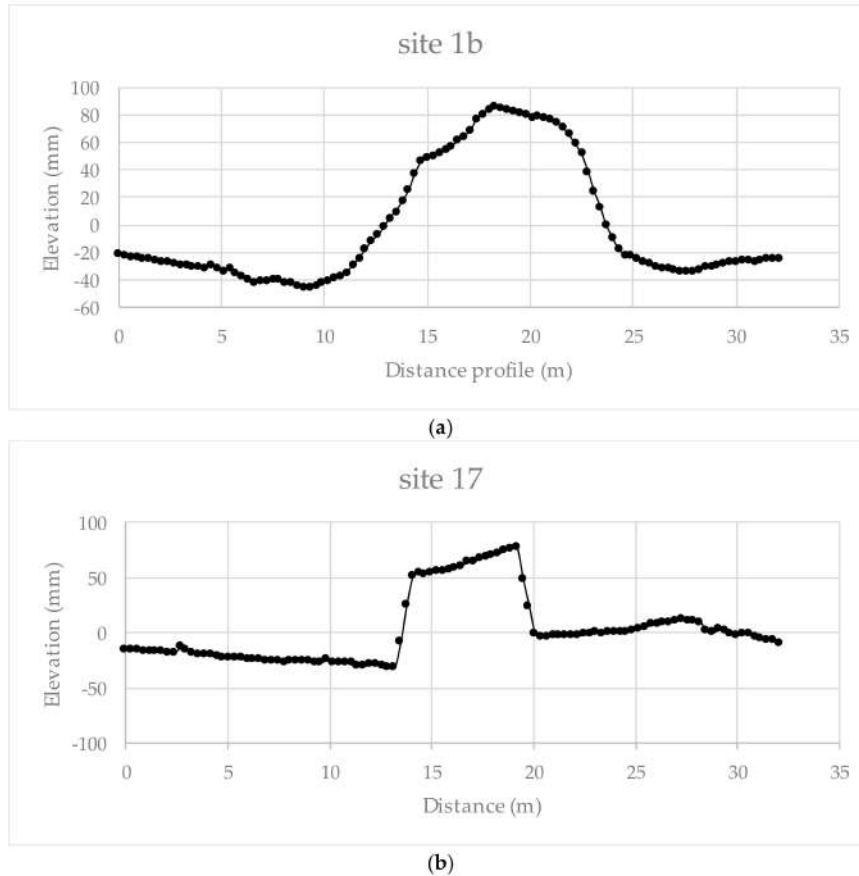


**Figure 6.** Example of measured longitudinal RPC profile: (a) site 1b; (b) site 17.

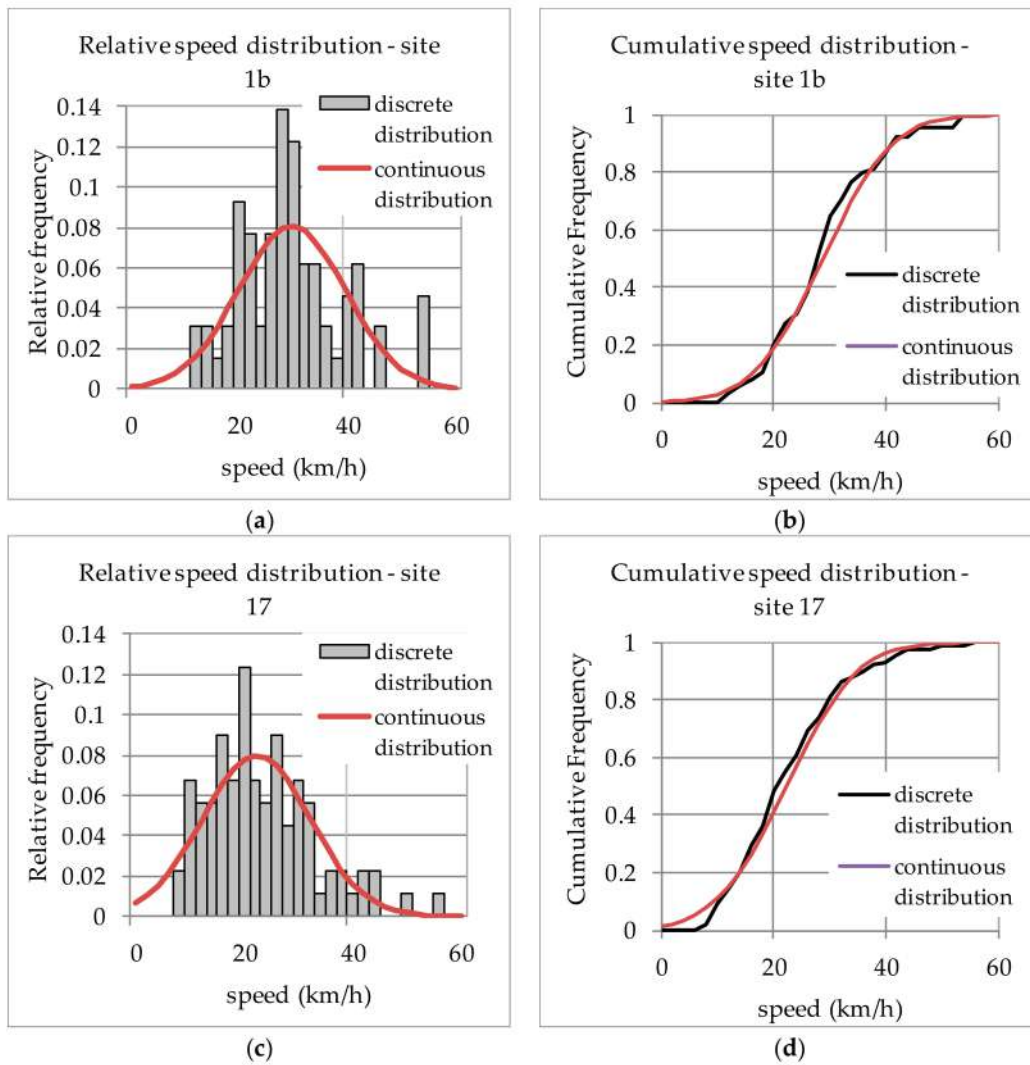


**Figure 7.** Empirical distribution of vehicle speed: (a) Frequency speed site 1b; (b) Cumulative frequency speed site 1b; (c) Frequency speed site 17; (d) Cumulative frequency speed site 17.



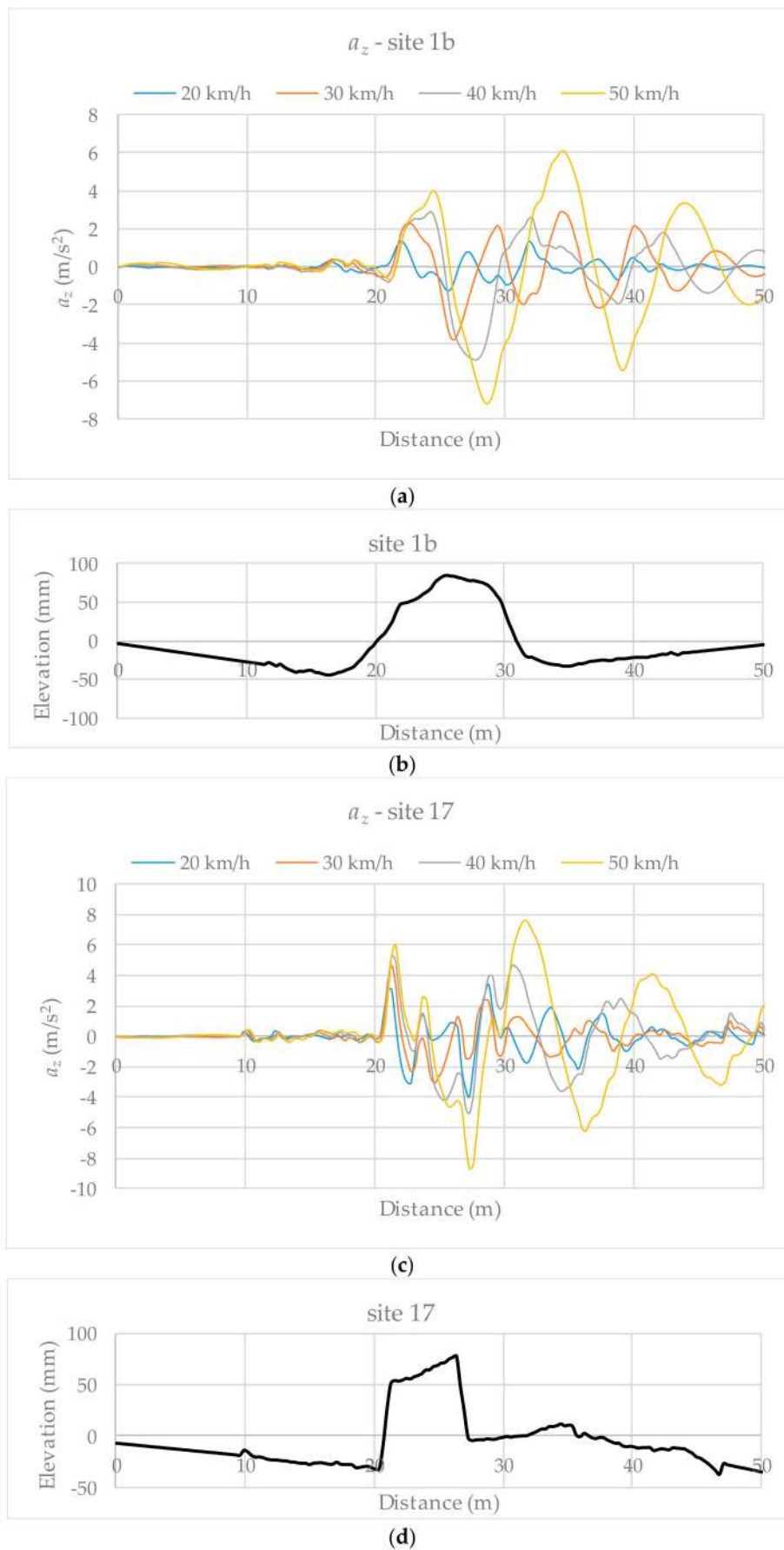


**Figure 8.** Calculated  $a_z$  experienced on board compared to longitudinal profile of the RPC: (a) Site1b  $a_z$  curve; (b) longitudinal profile of site 1b; (c) site 17  $a_z$  curve; (d) longitudinal profile of site 17.

Table 3 lists the obtained maximum and minimum values of  $a_z$  for car passengers passing through site 1b and site 17.

**Table 3.** Estimated maximum and minimum  $a_z$  on site 1b and site 17.

$v$ (km/h)	$a_z$ (m/s <sup>2</sup> )			
	Site 1b		Site 17	
	max	min	max	min
20	1.37	-1.24	3.38	-3.91
30	2.30	-3.85	4.67	-3.06
40	2.91	-4.88	5.27	-5.10
50	3.94	-7.21	7.60	-8.70

Given the results of each survey/survey site, an aggregate analysis of the collected data was carried out in order to investigate the characteristics of RPCs. Particularly, the relationships between the identified physical and geometrical characteristics (i.e., speed limit, inbound and outbound ramp slopes, elevation difference) have been examined.

The measurements from Dipstick have been processed in order to have symmetrical longitudinal profiles of the surveyed RPCs (Figure 9—some symbols will be explained after). The overall length  $L_t$  is composed of a two-branch approach curve where the parts are  $L_{a,1}$  and  $L_{a,2}$ , the flat top length  $L_c$ , and a two-branch exit curve where the parts are  $L_{e,1}$  and  $L_{e,2}$ . Particularly, approach and exit ramps have the same longitudinal slope (i.e.,  $i$ ) and length (i.e., the sag curves  $L_{a,1}$  and  $L_{e,1}$  have the same length, and the crest curves  $L_{a,2}$  and  $L_{e,2}$  have the same length). The flat top surface is parallel to the road pavement before and after the RPC (i.e., the RPC height is constant and equal to  $h$ ). Primary data about geometry of the surveyed RPCs are in the Supplementary Materials. Table 4 lists the results.

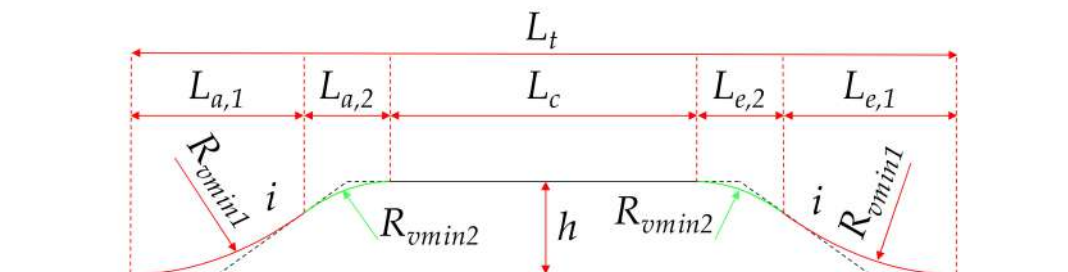


**Figure 9.** RPC longitudinal profiles.

**Table 4.** Geometric characteristics of surveyed RPCs.

$i$ (%)	Percentage of RPCs (%)	Number of RPCs	$h$ (cm)	Percentage of RPCs (%)	Number of RPCs
$0 < i < 2$	0.00%	0	$0 < h < 4$	0.00%	0
$2 \leq i < 3$	12.50%	3	$4 \leq h < 6$	20.83%	5
$3 \leq i < 4$	12.50%	3	$6 \leq h < 8$	8.33%	2
$4 \leq i < 5$	0.00%	0	$8 \leq h < 10$	33.33%	8
$5 \leq i < 6$	12.50%	3	$10 \leq h < 12$	20.83%	5
$6 \leq i < 7$	16.67%	4	$12 \leq h < 14$	0.00%	0
$7 \leq i < 8$	8.33%	2	$14 \leq h < 16$	4.17%	1
$8 \leq i < 9$	25.00%	6	$16 \leq h < 18$	4.17%	1
$9 \leq i < 10$	8.33%	2	$18 \leq h < 20$	0.00%	0
$10 \leq i < 11$	0.00%	0	$20 \leq h < 22$	8.33%	2
$11 \leq i < 12$	0.00%	0			
$12 \leq i < 13$	4.17%	1			

In Table 4 the majority of the RPCs have a slope between 5% and 10%, and are 4–12 cm high. Moreover, 4.17% and 12.50% of the surveyed RPCs do not fit the maximum longitudinal slope and the maximum sidewalk height (i.e., 10% and 15 cm, respectively) permitted by the Italian standard [47]. The obtained results highlight a great variety of configurations: Figure 10 represents the measured longitudinal profiles for roads where the administrative speed limit is 30 km/h.

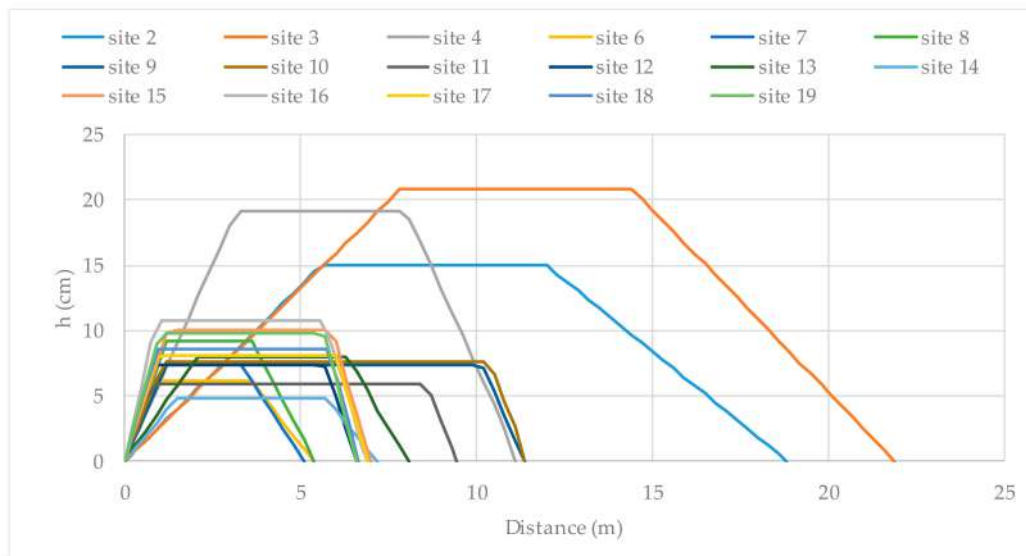


Figure 10. Longitudinal profiles for RPCs with 30 km/h administrative speed limit.

On the other hand, the normalization of profiles with respect to the RPC overall length points out the geometrical differences better: The curves in Figure 11 allow comparison qualitatively of the slopes of RPCs in Figure 10. Moreover, the values of the 85th percentile of measured speeds ( $v_{85}$ ) are reported because they are correlated with  $i$ : In most of the analyzed cases as slope index of the ramp increases, the speed of vehicles decreases. Figure 11 represents the measured longitudinal profiles for roads where the administrative speed limit is 30 km/h.

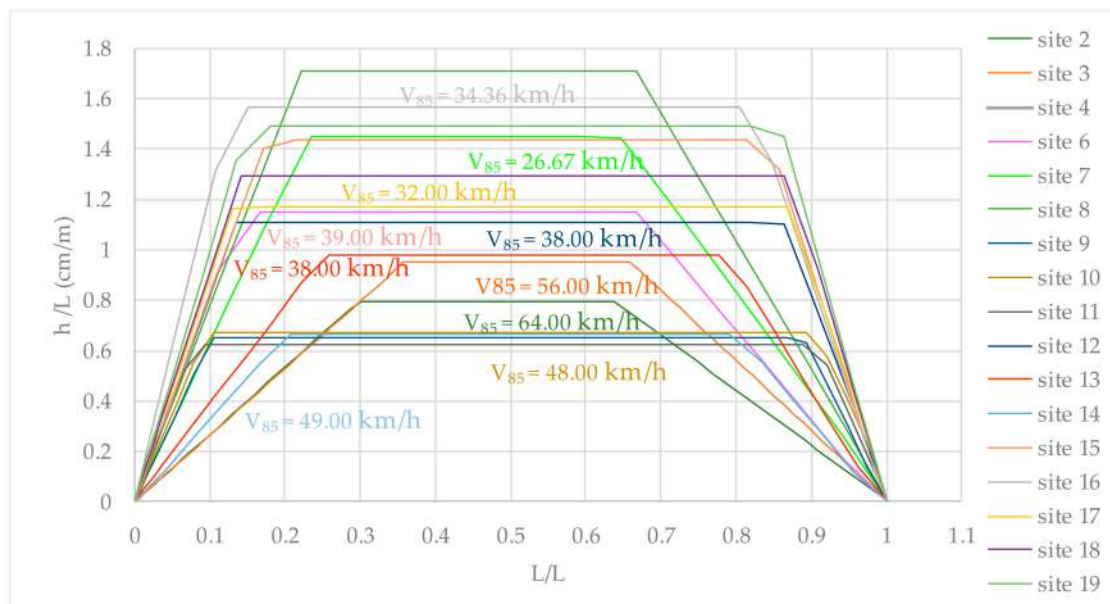
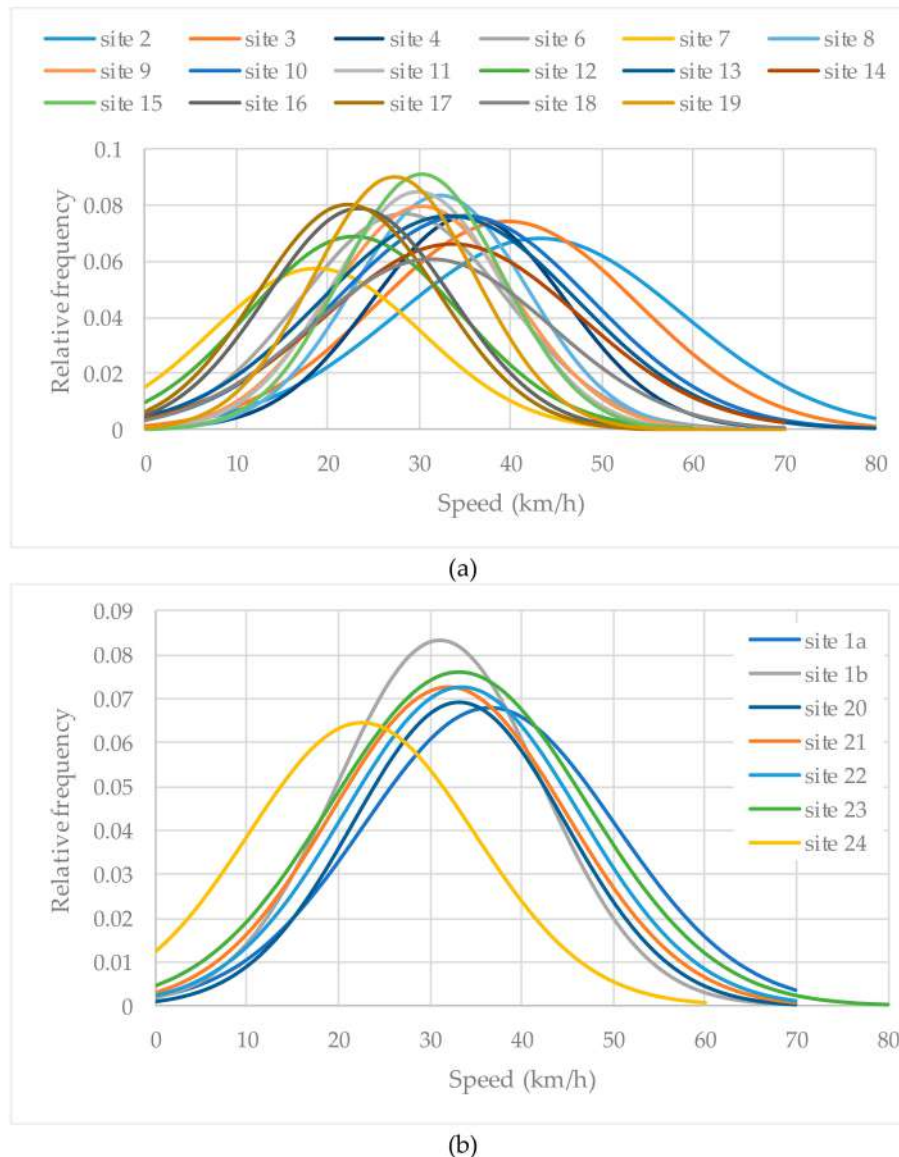


Figure 11. Normalization of longitudinal profiles for RPCs with 30 km/h administrative speed limit.

The geometric variability of RPCs affect distribution of measured vehicle speed: The lower the administrative speed level  $v$ , the higher the dispersion of measured speed values. Figure 12a,b allow comparison between RPCs with 30 km/h and 40 km/h administrative speed limit, respectively. Data about site 5 (administrative speed limit 40 km/h) are lacking.



**Figure 12.** Gaussian distribution of measured speed values for surveyed RPCs: (a) With 30 km/h administrative speed limit; (b) with 40 km/h administrative speed limit.

For administrative speed level equal to 30 km/h, the average values of measured speed are between 18 and 45 km/h, and the standard deviation increases with the increase of the average speed ( $v_a$ ). For administrative speed level equal to 40 km/h, both the average values and the standard deviation are comparable to each other. In Figure 12b, the blue curve differs from the others because of the non-correct geometry and non-adequate marking: Regular users of the road (site 24) limit their speed because they have experienced the RPCs and aim to prevent vehicle damage caused by contact with the pavement (e.g., grooves in Figure 5c,d).

It is therefore necessary to build RPCs according to geometrical standards, not overlooking functional requirements. Indeed, the calculation of  $a_z$  for different speed values revealed that vertical accelerations on the vehicle occupants are related to the longitudinal slope of the access ramp. Figure 13

shows a linear correlation between  $max a_z$  and  $i_a$ . The results in Figure 13 refer to all the observed 24 sites; data about the calculated vertical accelerations are available in the Supplementary Materials.

For each value of vehicle speed, the coefficient of determination  $R^2$  of the dashed trend lines is not less than 0.83.

Moreover, the longitudinal slope of access ramp affects the vehicle speed: For each surveyed site, both  $v_a$  and  $v_{85}$  decrease when  $i_a$  increases. Figure 14 refers to 16 RPCs (data about site 17 are lacking) where the speed limit is 30 km/h: A similar logarithmic trend has been observed when  $v$  is 40 km/h.

Finally, the dynamic analysis of vehicle passage revealed that there is no correlation between  $max a_z$  and  $h_m$ , as confirmed by Figure 15. The results in Figure 15 refer to all the observed 24 sites.

However, the high values of  $max a_z$  in Figure 15 highlight that often the surveyed RPCs are used for traffic calming. Particularly, 99% of the simulated passages induce a vertical acceleration on occupants higher than  $0.6 \text{ m/s}^2$ , which is the maximum value permitted by [47] for comfort reasons. Therefore, this value has been adopted as one of the examined criteria to design RPCs.

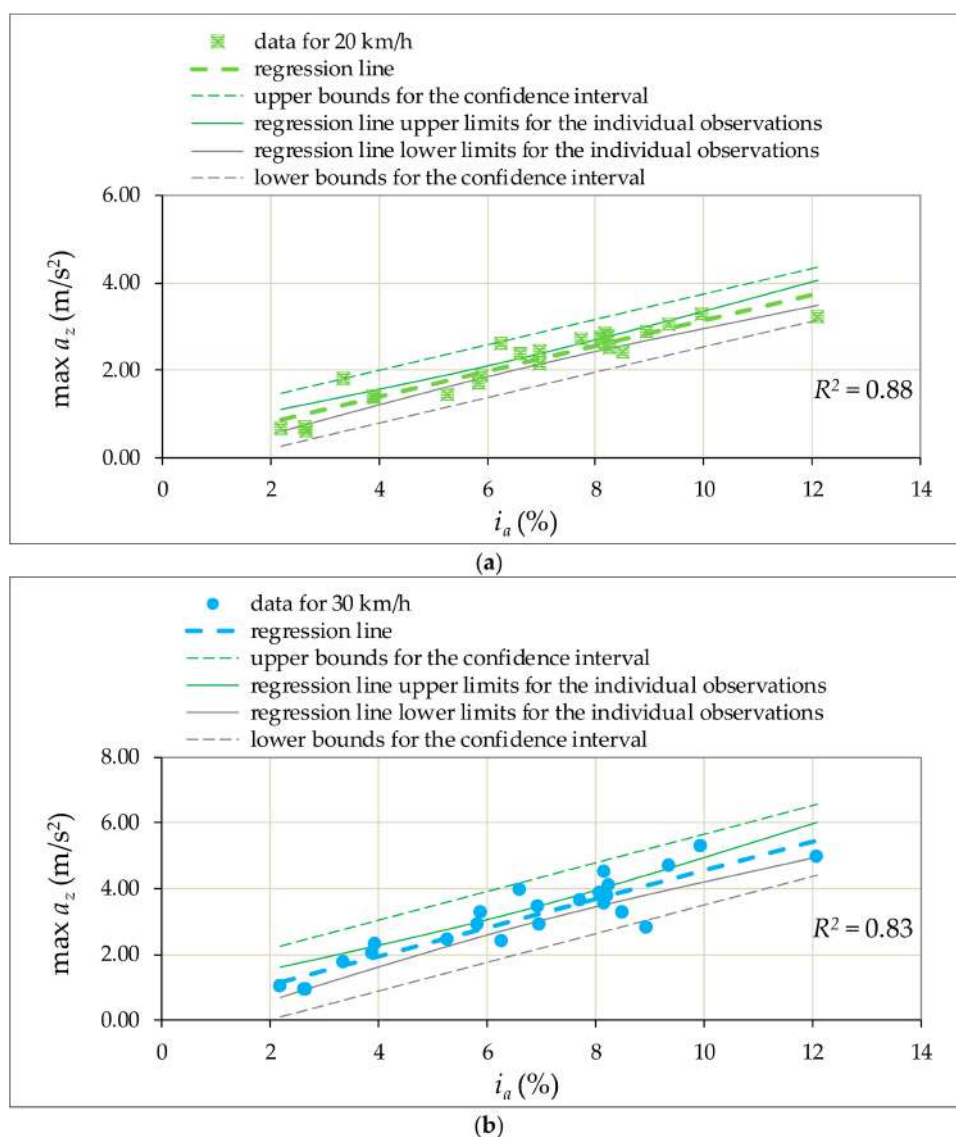
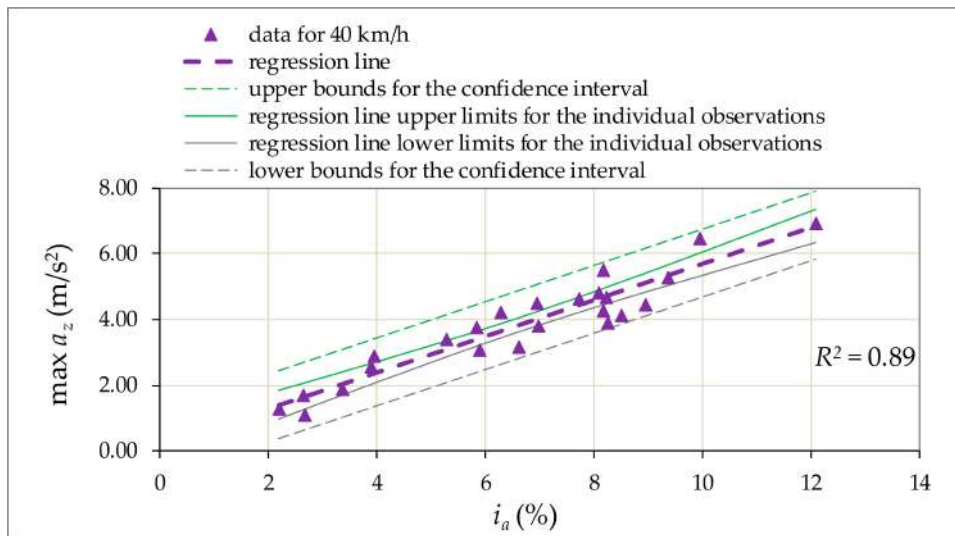
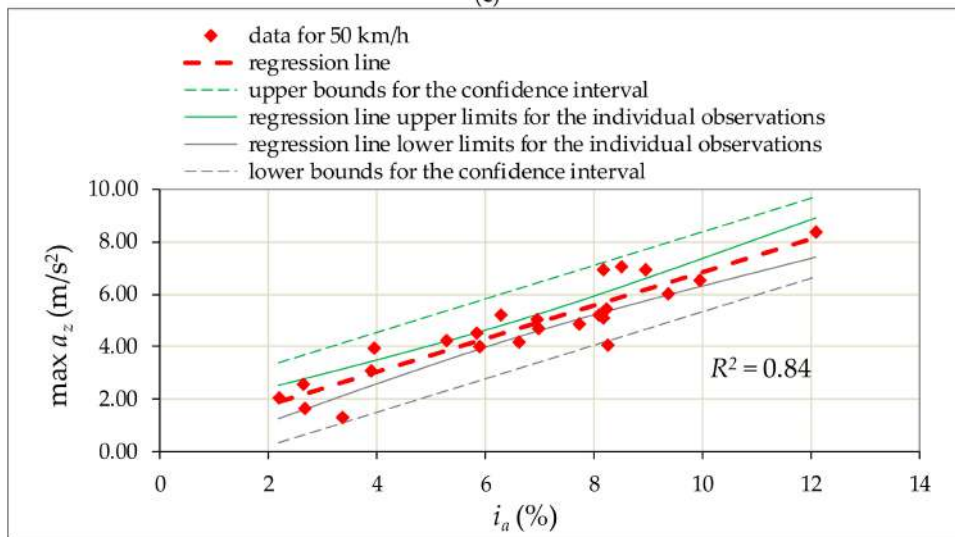


Figure 13. Cont.



(c)



(d)

**Figure 13.** Correlation between  $i_a$  and  $a_z$  for different speed values: (a) 20 km/h; (b) 30 km/h; (c) 40 km/h; (d) 50 km/h.

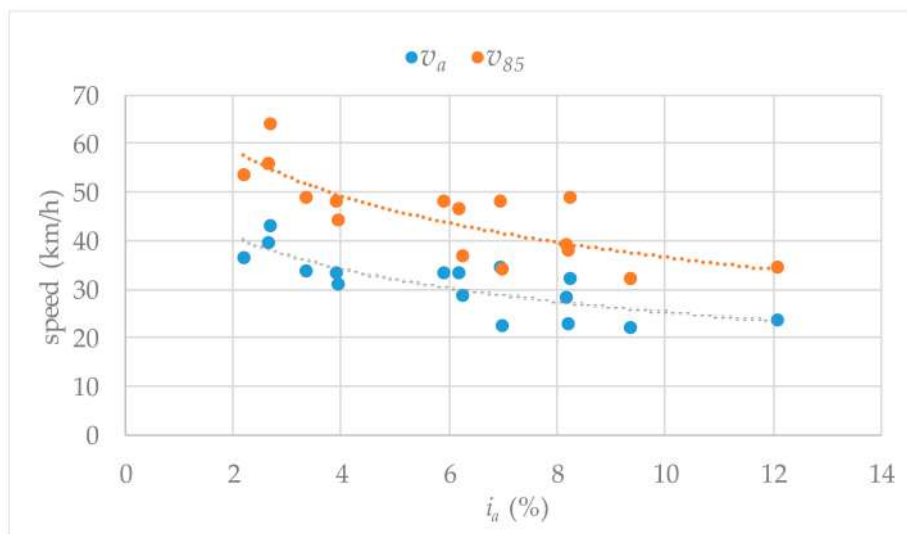


**Figure 14.** Correlation between  $i_a$  and vehicle speed.

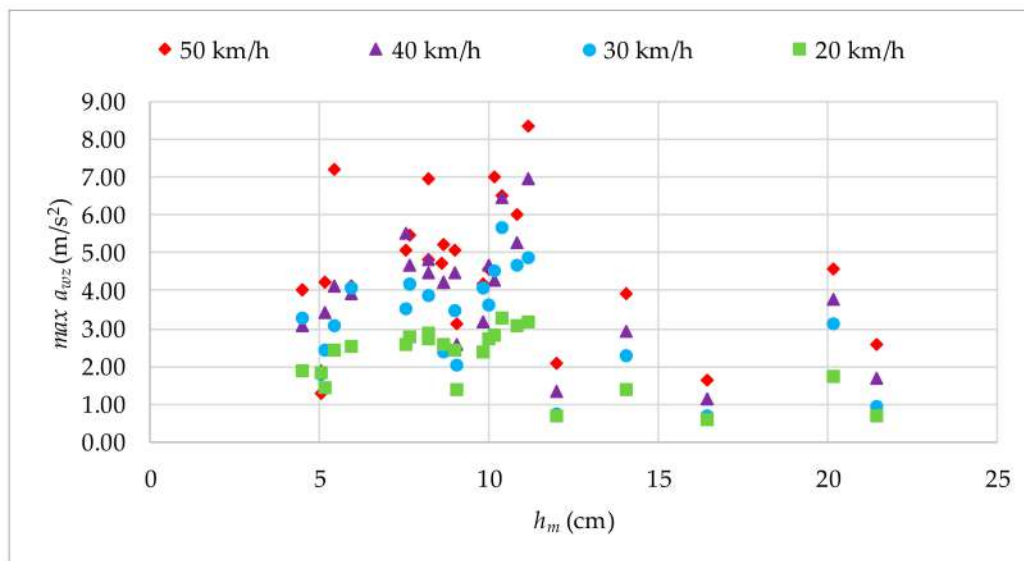


Figure 15. Correlation between  $h_m$  e and  $max a_z$ .

#### 4. Discussion

In regards to Figure 9, in the post-processing phase, the authors assumed two design approaches: The first one complies with the Italian standards about geometrical rules to design roads [47], and the second one complies with the Italian driving code [48].

The first approach assumes that RPCs are routes across carriageways raised to the same level, or close to the same level, as the sidewalks that provide access to the pedestrian crossing. Therefore, they do not have traffic-calming purposes. Three conditions should be filled: The contact between any part of the reference vehicle and the pavement should be avoided, the ride comfort experienced by driver and passengers should be guaranteed limiting the vertical acceleration, and the stopping (for crest curves) and heading (for sag curves) sight distance should be verified.

In order to avoid contact between vehicle and pavement, geometrical criteria are defined by [49] to design crest and sag vertical curves: The minimum vertical radius is 20 m ( $R_{vmin2}$ ) and 40 m ( $R_{vmin1}$ ), respectively. Therefore, the absolute value of the maximum value of the vertical acceleration over a crest is higher than that over a sag: It is because of the different value of the permitted minimum vertical radius ( $R_{vmin}$ ). Given the same vehicle speed and the minimum permitted value of the vertical radius, the vertical acceleration over a crest is double than over a sag (Equation (2)).

Given the two values of  $R_{vmin1}$  and  $R_{vmin2}$ , for three values of  $h$  (i.e., 5, 10, and 15 cm), the values of the maximum  $i$  and  $L_a, L_e, L_f$  have been calculated according to Equations (2)–(8).

$$L_{a,2} = L_{e,2} = R_{vmin2} \frac{i}{100} = 20 \frac{i}{100} \text{ (crest curves)} \tag{2}$$

$$L_{a,1} = L_{e,1} = R_{vmin1} \frac{i}{100} = 40 \frac{i}{100} \text{ (sag curves)} \tag{3}$$

$$h = L_A \frac{i}{100} = \left( \frac{L_{a,1}}{2} + \frac{L_{a,2}}{2} \right) \frac{i}{100} = L_E \frac{i}{100} = \left( \frac{L_{e,1}}{2} + \frac{L_{e,2}}{2} \right) \frac{i}{100} \tag{4}$$

The total length of the RPC has been calculated according to Equation (4):

$$L_t = L_a + L_c + L_e = L_a + L_f + L_e - L_{a,2} \tag{5}$$

having the conditions given by Equations (5)–(7):

$$L_a = L_{a,1} + L_{a,2} = L_e = L_{e,1} + L_{e,2} \tag{6}$$

$$i = i_a = i_e = \sqrt{\frac{20000 h}{R_{vmin1} + R_{vmin2}}} \tag{7}$$

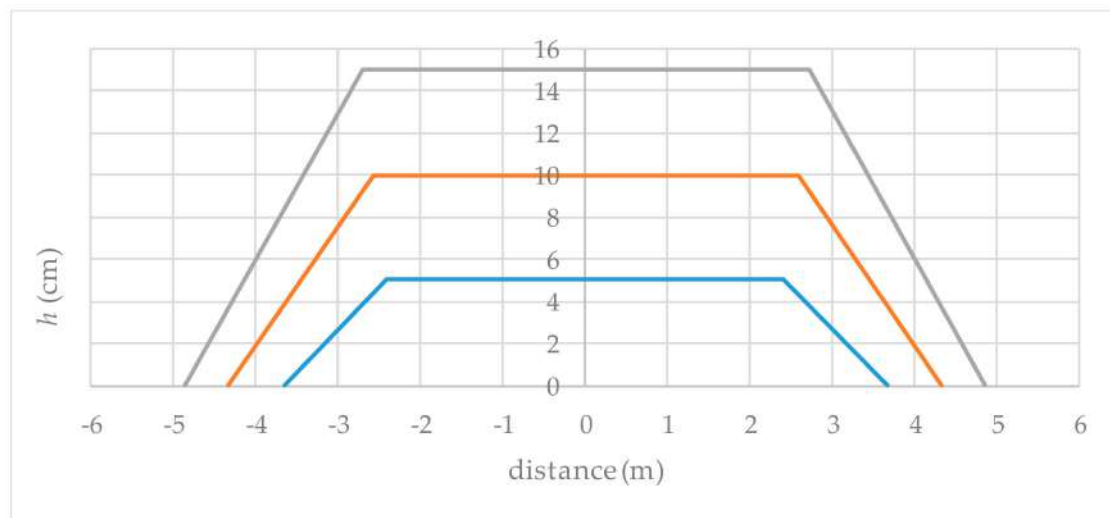
$$L_c = 4 \text{ m} \tag{8}$$

Table 5 lists the results.

**Table 5.** Geometric characteristics of RPCs designed with a traffic-calming purpose criterion.

<i>h</i> (cm)	<i>i</i> (%)	<i>L<sub>a</sub></i> (m)	<i>L<sub>A</sub></i> (m)	<i>L<sub>f</sub></i> (m)	<i>L<sub>e</sub></i> (m)	<i>L<sub>t</sub></i> (m)
5	4.08	2.45	1.23	4.82	2.45	8.90
10	5.77	3.46	1.73	5.15	3.46	10.93
15	7.07	7.07	4.24	5.41	7.07	12.49

The obtained values give the longitudinal profiles in Figure 16: According to the geometric criteria, the ramp slope increases with increasing *h*.



**Figure 16.** Schemes of RPCs longitudinal profiles—geometric criterion.

The results from the implementation of the proposed geometric criteria have been compared to each surveyed site: 29.2% of the sites satisfy the limits of *i* (i.e., site 1a, 1b, 2, 3, 4, 13, and 14).

In order to satisfy the comfort ride criterion, given the maximum vertical acceleration (*a<sub>vlim</sub>*) laid down by [47], for three administrative speed limits (i.e., 20, 30 and 40 km/h) and three values of *h* (i.e., 5, 10, and 15 cm), the values of *i*, *R<sub>vmin</sub>*, *L<sub>a</sub>*, and *L<sub>e</sub>* (Figure 9) have been calculated according to Equations (2)–(8) and Equation (9):

$$R_{vmin} = v^2 / (12.96 \times a_{vlim}) \tag{9}$$

where *v* is the administrative speed limit and *a<sub>vlim</sub>* is equal to 0.6 m/s<sup>2</sup>.

Table 6 lists the geometric characteristics of RPCs according to the comfort criterion.

The values in Table 6 give the longitudinal profiles in Figure 17.

The longitudinal profiles in Figure 17 reveal that:

- For a given value of *h*, the comfort reasons imply longer RPCs than geometrical constrains (i.e., for *h* = 15 cm *L<sub>t</sub>* ranges between 15.11 m and 31.78 m according to the comfort criterion, while *L<sub>t</sub>* is 12.49 m according to the geometrical criterion). Since both criteria should be fulfilled, the most restrictive should be considered to correctly design an RPC;
- For a given value of *h*, the slope decreases with increasing the vehicle speed;



- For a given value of  $v$ , the slope increases with increasing value of  $h$ .

According to the calculated  $R_{vmin}$ , Figure 18 shows the longitudinal profile of an RPC having  $v$  equal to 30 km/h and  $h$  equal to 15 cm.

**Table 6.** Geometric characteristics of RPCs according to the comfort criterion.

$v$ (km/h)	$R_{vmin}$ (m)	$h$ (cm)	$i$ (%)	$L_a$ (m)	$L_A$ (m)	$L_f$ (m)	$L_e$ (m)	$L_t$ (m)
20	51.44	5	3.12	3.21	1.60	5.60	3.21	10.41
		10	4.41	4.54	2.27	6.27	4.54	13.07
		15	5.40	5.56	2.78	6.78	5.56	15.11
30	115.75	5	2.08	4.81	2.41	6.41	4.81	13.62
		10	2.94	6.80	3.40	7.40	6.80	17.61
		15	3.60	8.33	4.17	8.17	8.33	20.67
40	205.75	5	1.56	6.41	3.21	7.21	3.21	16.83
		10	2.20	9.07	4.54	8.54	4.54	22.14
		15	2.70	11.11	5.56	9.56	5.56	26.22
50	321.50	5	1.25	8.02	4.01	8.01	8.02	20.04
		10	1.76	11.34	5.67	9.67	11.34	26.68
		15	2.16	13.89	6.94	10.64	13.89	31.78

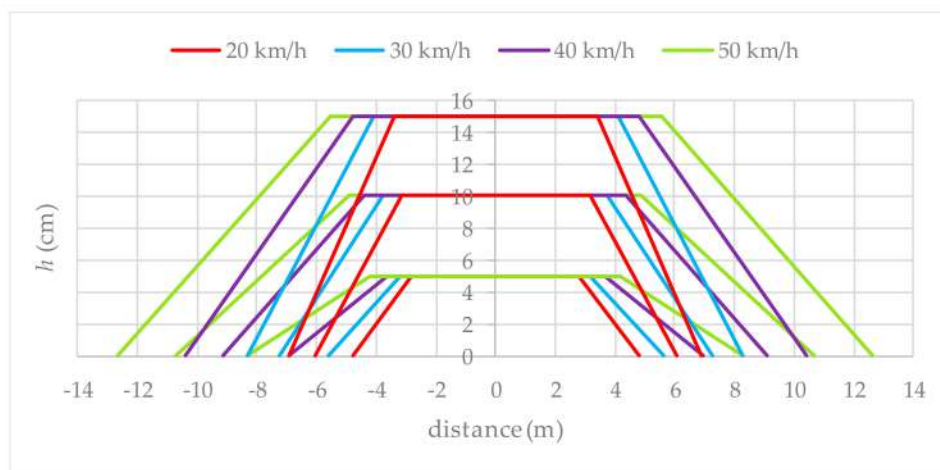


**Figure 17.** Schemes of RPCs longitudinal profiles—comfort criterion.

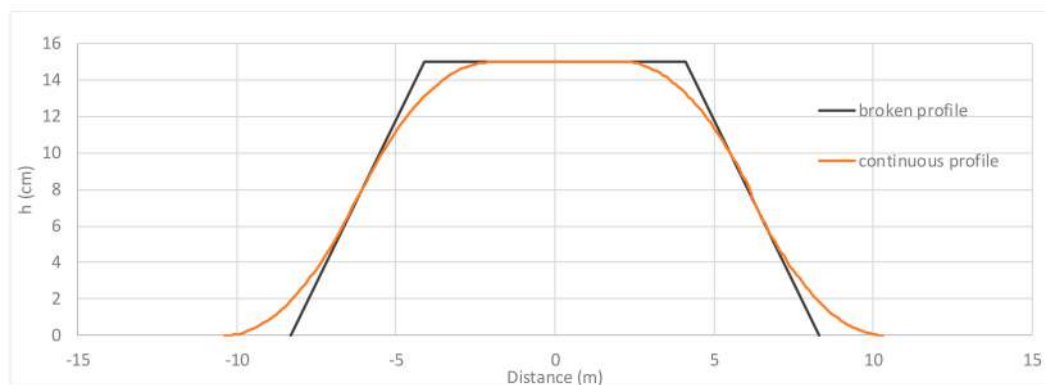


**Figure 18.** Longitudinal profile of RPC having  $v = 30$  km/h and  $h = 15$  cm.

The results from the implementation of the proposed comfort criterion have been compared to each relieved RPC: For each surveyed site, Table 7 lists the effective and theoretical geometry of the RPCs.

**Table 7.** Comparison between relieved profiles and RPCs designed according to the comfort criterion.

<i>v</i> (km/h)	Site ID	Effective Geometry			Geometrical Limits		Verification
		<i>h</i> (cm)	<i>i<sub>a</sub></i> (%)	<i>i<sub>e</sub></i> (%)	<i>R<sub>v min</sub></i> (m)	<i>i<sub>max</sub></i> (%)	<i>i<sub>max</sub></i> > Average ( <i>i<sub>a</sub></i> ; <i>i<sub>e</sub></i> )
30	site 14	5.06	3.36	3.55	115.75	2.09	no
	site 6	7.56	8.17	3.56		2.56	no
	site 12	7.66	8.22	7.88		2.57	no
	site 18	8.19	8.95	10.58		2.66	no
	site 11	8.24	8.09	6.77		2.67	no
	site 7	8.65	6.27	4.02		2.73	no
	site 10	8.99	6.96	6.59		2.79	no
	site 13	9.03	3.90	4.97		2.79	no
	site 9	9.84	6.61	5.93		2.92	no
	site 8	10.00	7.73	5.07		2.94	no
	site 15	10.18	8.17	9.41		2.97	no
	site 19	10.36	9.96	10.74		2.99	no
	site 17	10.85	9.36	8.65		3.06	no
	site 16	11.14	12.10	8.94		3.10	no
	site 2	16.44	2.68	2.19		3.77	yes
	site 4	20.16	5.84	5.94		4.17	no
site 3	21.45	2.65	2.78	4.30	yes		
40	site 23	4.47	5.89	7.75	205.75	1.47	no
	site 20	5.19	5.27	6.10		1.59	no
	site 5	5.41	9.75	9.72		1.62	no
	site 22	5.43	8.50	6.12		1.62	no
	site 21	5.93	8.25	6.56		1.70	no
	site 24	8.59	6.98	9.67		2.04	no
	site 1a	11.99	2.20	3.56		2.41	no
	site 1b	14.08	3.94	3.82		2.62	no

According to the data in Table 8, more than 90% of the surveyed RPCs do not comply with the limits of the ramp longitudinal slope. Such conditions imply that ride comfort is not guaranteed, and the RPCs do not comply with the Italian geometric rules about road design.

**Table 8.** Geometric characteristics of speed tables.

<i>v</i> (km/h)	Maximum Value	Minimum Values			
	<i>h</i> (cm)	<i>L<sub>a</sub></i> (m)	<i>L</i> (m)	<i>L<sub>e</sub></i> (m)	<i>L<sub>T</sub></i> (m)
20		not declared			
30	7	4	4	4	12
40	5	3	3	3	9
50	3	2	2	2	6

The last criterion, about the verification of the stopping sight distance, is always verified. Given the driver’s eye height is equal to 1.10 m, and the object height equal to 0.10 m, the RPC (in the study it is not more than 15 cm high) does not obstruct the driver’s line of sight.

Therefore, only site 2 and site 3 (i.e., less than 9% of the overall surveyed RPCs) comply with the Italian geometrical and functional criteria to design roads (and pedestrian crossings).

Finally, the second approach consists of a pedestrian crossing on a midblock traffic-calming device that raises the entire wheelbase of a vehicle to reduce its traffic speed. Therefore, an RPC joins two objectives: To have a raised feature, and to slow the speed of approaching vehicles. Under such conditions, RPCs also perform the tasks assigned to traffic-calming devices (e.g., speed tables, speed humps, or speed bumps). Figure 19 represents a black and yellow speed table according to [49]: It is trapezoidal in shape with sharp edges of the inclined ramp.



Figure 19. Example of speed table.

The regulation implementing the Italian driving code [49] provides geometries of features that are permitted on residential roads and living streets, but they are banned on lifelines. Table 8 lists the geometric constraints of a trapezoidal speed table.

The longitudinal profiles obtained from limits in Table 8 allowed for the calculation of  $a_{wz}$  using the full car model: Table 9 summarizes the results.

Table 9.  $a_{wz}$  values caused by a speed table.

$v$ (km/h)	$a_{wz}$ (m/s <sup>2</sup> )
20	-
30	6.06
40	4.14
50	1.98

The comparison between the values of  $a_{wz}$  obtained from surveys and calculated for speed tables highlights that two RPCs (i.e., site 1a and site 1b) do not comply with geometrical and dynamic criteria for speed tables (Table 10).

Table 10. Values of  $a_{wz}$  on the surveyed RPCs and on the designed speed tables.

$v$ (km/h)	RPC	$a_{wz}$ (m/s <sup>2</sup> )		
		Surveyed RPCs	Designed Speed Table	
30	site 2	0.70		
	site 3	0.93		
	site 4	3.13		
	site 6	3.54		
	site 7	2.37		
	site 8	3.62		
	site 9	4.06		
	site 10	3.46		
	site 11	3.89	6.06	
	site 12	4.18		
	site 13	2.02		
	site 14	1.77		
	site 15	4.50		
	site 16	4.86		
	site 17	4.67		
	site 18	2.79		
	site 19	5.68		
	40	site 1a	4.26	
		site 1b	4.18	
site 5		3.64		
site 20		3.90		
site 21		3.42	4.14	
site 22		4.12		
site 23		3.08		
site 24		3.80		

The following observations were made concerning the collected data and the adopted criteria:

- For a given value of  $h$ , RPCs designed with the geometric criterion imply lower values of  $L_t$  than ones designed with the comfort criterion. It implies that when  $h$  is 15 cm the maximum value of  $a_z$  reaches 3.47 m/s<sup>2</sup> and 6.17 m/s<sup>2</sup> when the vehicle passes over the crest with a speed of 30 km/h and 40 km/h, respectively;
- $i_{max}$  increases with the increase of  $h$  (i.e., the height of the sidewalk) regardless of the adopted criterion (Figures 16 and 17);
- Experimental data show that the greater the longitudinal slope  $i_a$  is, the lower the average speed will be (Figure 14). However, RPCs do not have (if properly designed) traffic-calming effects because they are the only features that allow pedestrians to cross the road without having to step onto the road itself;
- In regards to the Italian standards, less than 9% of the surveyed RPCs fit the criteria to design roads (i.e., site 2 and 3), while more than 90% of them comply with the traffic-calming criterion for designing speed tables (site 1a and 1b induce a vertical acceleration on occupants higher than the maximum value permitted for speed table features);
- The lack of regulation on geometrical and functional criteria for designing these raised pedestrian crossings result in an extreme variation: Effectiveness of these treatments is not guaranteed.

The observed differences in terms of geometrical characteristics of longitudinal profiles and induced vertical accelerations highlight that two different approaches could be pursued to design RPCs, and they cannot be mixed:

- Raised devices to enhance accessibility at crossing: The longitudinal profile of the RPC should comply with geometrical and functional criteria for designing roads. According to the Italian standard [47], the minimum vertical radius of crest and sag curves is 20 m and 40 m, respectively; the maximum the maximum vertical acceleration induced to vehicle occupants is 0.6 m/s<sup>2</sup>. Therefore, this device has no application limits related to road type;
- Speed tables to reduce vehicle speeds (and to enhance the pedestrian environment) at crossings: It is not appropriate for bus routes or emergency routes because of the vertical accelerations induced for vehicle occupants. SCUs are traffic-calming units and aim to reduce noise and pollution from traffic in residential, local, or collector roads where the administrative speed limit is lowered compared to the ordinary administrative speed limit.

## 5. Conclusions

Road design should focus on vulnerable users, particularly when different types of users share the space. Pedestrian crossings are among the most critical road sections, where motorized vehicles and pedestrians interact.

This paper starts from geometrical and cinematic reliefs carried out on twenty-four RPCs in urban areas: These activities consisted of the visual survey, the measurement of geometric characteristics of 24 RPCs through a hand-held Dipstick road profiler, and the measurement of the vehicle speed through two infrared sensors. The collected data were analyzed to calculate the whole-body vibration acceleration induced for vehicle occupants while they are passing over. In the post-processing analysis, two geometrical and functional approaches to design RPCs have been considered: Both derive from Italian standards. In the first one, RPC provides a designated route across carriageways raised to the same level, or close to the same level, as the sidewalks that provide access to the pedestrian crossing; in the second one, RPC acts as both a marked pedestrian feature and a traffic-calming device (i.e., SCU).

Regarding the first approach, both geometrical and comfort criteria should be satisfied: The comfort reasons are more restrictive than geometrical constrains. For a given  $h$  value, the overall length of an RPC is longer when satisfying the comfort criterion rather than the geometrical one. Moreover,  $L_t$  depends on the administrative speed limit: The higher the value of  $v$ , the longer the value of  $L_t$ .

Therefore, for  $h = 10$  cm and  $v$  between 20 and 50 km/h,  $L_t$  ranges between 13.07 m and 26.68 m according to the comfort criterion, while it is 10.93 m according to the geometrical criterion. Since both criteria should be fulfilled, the most restrictive (i.e., comfort criterion which limits the on-board vertical accelerations at a maximum of  $0.6 \text{ m/s}^2$ ) should be considered to correctly design an RPC. The comparison between the standard limits for designing RPCs and the data obtained from surveys revealed that less than 9% of the surveyed sites comply with the considered criteria.

In regards to the second approach (i.e., pedestrian crossings as traffic-calming), it is permitted on residential roads and living streets, but it is banned on lifelines. The design of speed tables requires high values of the maximum vertical accelerations (i.e.,  $6.06 \text{ m/s}^2$ ,  $4.14 \text{ m/s}^2$ , and  $1.98 \text{ m/s}^2$  for 30 km/h, 40 km/h, and 50 km/h, respectively) in order to induce a speed reduction. More than 90% of the surveyed RPCs' comfort ride conditions are within the limits laid down for speed tables. However, they are on urban roads where bus and emergency traffic pass, indicating they're not correctly designed.

The results of this study highlight that the lack of regulation opens up several very different features. Therefore, it is necessary to identify and define strategic priorities concerning management of urban pedestrian crossings to improve the safety level. For this purpose, geometrical and functional analyses should be carried out to identify the best strategies and overcome the regulation gap in this subject.

**Supplementary Materials:** The following are available online at <http://www.mdpi.com/2076-3417/9/14/2844/s1>, primary data about geometry (see Figures 2 and 9) and obtained vertical acceleration values (see Figure 13): Sheet primary data; relieved longitudinal profiles of each RPC: Sheets site N (with N ranging between 1 and 24).

**Author Contributions:** Conceptualization, G.L.; formal analysis, E.B.; funding acquisition, E.B.; investigation, E.B.; methodology, G.L. and E.B.; software, G.L.; validation, G.L., L.M., A.P., and E.B.; writing—original draft, G.L., L.M., and A.P.; writing—review & editing, G.L., L.M., and A.P.

**Funding:** This research received no external funding.

**Acknowledgments:** The authors thank Eng. Roberto Oliverio who conceived and constructed the self-made device in Figure 1a.

**Conflicts of Interest:** The authors declare no conflict of interest.

## References

1. World Health Organization. *Pedestrian Safety: A Road Safety Manual for Decision-Makers and Practitioners*; World Health Organization: Geneva, Switzerland, 2013.
2. Antić, B.; Pešić, D.; Vujanić, M.; Lipovac, K. The influence of speed bumps heights to the decrease of the vehicle speed—Belgrade experience. *Saf. Sci.* **2013**, *57*, 303–312. [[CrossRef](#)]
3. Onelcin, P.; Alver, Y. The crossing speed and safety margin of pedestrians at signalized intersections. *Transp. Res. Procedia* **2017**, *22*, 3–12. [[CrossRef](#)]
4. Berloco, N.; Colonna, P.; Intini, P.; Masi, G.; Ranieri, V. Low-cost smartphone-based speed surveying methods in proximity to traffic calming devices. *Procedia Comput. Sci.* **2018**, *134*, 415–420. [[CrossRef](#)]
5. Gonzalo-Orden, H.; Pérez-Acebo, H.; Unamunzaga, A.L.; Arce, M.R. Effects of traffic calming measures in different urban areas. *Transp. Res. Procedia* **2018**, *33*, 83–90. [[CrossRef](#)]
6. Gitelman, V.; Carmel, R.; Pesahov, F.; Chen, S. Changes in road-user behaviors following the installation of raised pedestrian crosswalks combined with preceding speed humps, on urban arterials. *Transp. Res. F Traffic Psychol. Behav.* **2017**, *46*, 356–372. [[CrossRef](#)]
7. Demasi, F.; Loprencipe, G.; Moretti, L. Road Safety Analysis of Urban Roads: Case Study of an Italian Municipality. *Safety* **2018**, *4*, 58. [[CrossRef](#)]
8. Ragnoli, A.; Corazza, M.V.; Di Mascio, P. Safety ranking definition for infrastructures with high PTW flow. *J. Traffic Transp. Eng.* **2018**, *5*, 406–416. [[CrossRef](#)]
9. Ragnoli, A.; Corazza, M.V.; Di Mascio, P.; Musso, A. Maintenance priority associated to powered two-wheeler safety. *WIT Trans. Built Environ.* **2018**, *176*, 453–464.
10. Cantisani, G.; Moretti, L.; De Andrade Barbosa, Y. Safety Problems in Urban Cycling Mobility: A Quantitative Risk Analysis at Urban Intersections. *Safety* **2019**, *5*, 6. [[CrossRef](#)]

11. Cantisani, G.; Moretti, L.; De Andrade Barbosa, Y. Safety Risk Analysis and Safer Layout Design Solutions for Bicycles in Four-Leg Urban Intersections. *Safety* **2019**, *5*, 24. [CrossRef]
12. Di Mascio, P.; Fusco, G.; Grappasonni, G.; Moretti, L.; Ragnoli, A. Geometrical and functional criteria as a methodological approach to implement a new cycle path in an existing Urban Road Network: A Case study in Rome. *Sustainability* **2018**, *10*, 2951. [CrossRef]
13. Wood, D.P.; Simms, C.; Walsh, D. Vehicle-pedestrian collisions: Validated models for pedestrian impact and projection. *Proc. Inst. Mech. Eng. D J. Automob. Eng.* **2005**, *219*, 183–195. [CrossRef]
14. Kırbaşı, U.; Karaşahin, M. Comparison of Speed Control Bumps and Humps according to Whole-Body Vibration Exposure. *J. Transp. Eng. Part A Syst.* **2018**, *144*, 04018054. [CrossRef]
15. Corazza, M.V.; Di Mascio, P.; Moretti, L. Management of sidewalk maintenance to improve walking comfort for senior citizens. *WIT Trans. Built Environ.* **2018**, *176*, 195–206.
16. Corazza, M.V.; Di Mascio, P.; Moretti, L. Managing sidewalk pavement maintenance: A case study to increase pedestrian safety. *J. Traffic Transp. Eng.* **2016**, *3*, 203–214. [CrossRef]
17. Jägerbrand, A.; Johansson, M.; Laike, T. Speed Responses to Speed Humps as Affected by Time of Day and Light Conditions on a Residential Road with Light-Emitting Diode (LED) Road Lighting. *Safety* **2018**, *4*, 10. [CrossRef]
18. FHWA. *Methods and Practices for Setting Speed Limits: An Informational Report*. FHWA-SA-12-004; Federal Highway Administration: Washington, DC, USA, 2012.
19. Transportation Research Board. *Managing Speed: Review of Current Practice for Setting and Enforcing Speed Limit. Special Report 254*; National Academy of Sciences: Washington, DC, USA, 1998.
20. Statistical analysis of geometric characteristics and speed reductions for raised pedestrian crosswalks (RPC). Available online: <https://www.tandfonline.com/doi/ref/10.1080/19439962.2018.1490366?scroll=top> (accessed on 7 December 2018).
21. Lopez Lambas, M.E.; Corazza, M.V.; Monzon, A.; Musso, A. Rebalancing urban mobility: A tale of four cities. *Urban Des. Plan.* **2013**, *166*, 274–287. [CrossRef]
22. Corazza, M.V.; Favaretto, N. A Methodology to Evaluate Accessibility to Bus Stops as a Contribution to Improve Sustainability in Urban Mobility. *Sustainability* **2019**, *11*, 803. [CrossRef]
23. Sgarra, V.; Di Mascio, P.; Corazza, M.V.; Musso, A. An application of ITS devices for powered two-wheelers safety analysis: The Rome case study. *Adv. Transp. Stud.* **2014**, *33*, 85–96.
24. Corazza, M.V.; Musso, A.; Finikopoulos, K.; Sgarra, V. An analysis on health care costs due to accidents involving powered two wheelers to increase road safety. *Transp. Res. Procedia* **2016**, *14*, 323–332. [CrossRef]
25. Litman, T. *Traffic Calming: Benefits, Costs and Equity Impacts*; Victoria Transport Policy Institute Victoria: Victoria, BC, Canada, 1999.
26. Pau, M.; Angius, S. Do speed bumps really decrease traffic speed? An Italian experience. *Accid. Anal. Prev.* **2001**, *33*, 585–597. [CrossRef]
27. Parkhill, M.; Sooklall, R.; Bahar, G. Updated guidelines for the design and application of speed humps. In *ITE 2007 Annual Meeting and Exhibit*; Institute of Transportation Engineers: Pittsburgh, PA, USA, 2007.
28. Fwa, T.; Liaw, C. Rational approach for geometric design of speed-control road humps. *Transp. Res. Rec.* **1992**, *66*, 72.
29. Salau, T.A.O.; Adeyefa, A.O.; Oke, S.A. Vehicle speed control using road bumps. *Transport* **2004**, *19*, 130–136. [CrossRef]
30. Aghazadeh, B.S.; Saeedi, K.; Yazdi, M.R.H. Simulation of ride quality of vehicles crossing road humps. In *Proceedings of the International Conference on Modeling and Simulation*, Konya, Turkey, 28–30 August 2006.
31. Patel, T.; Vasudevan, V. Impact of speed humps of bicyclists. *Saf. Sci.* **2016**, *89*, 138–146. [CrossRef]
32. Pedersen, N.L. Shape optimization of a vehicle speed control bump. *J. Struct. Mech.* **1998**, *26*, 319–342. [CrossRef]
33. Khorshid, E.; Alkalby, F.; Kamal, H. Measurement of whole-body vibration exposure from speed control humps. *J. Sound Vib.* **2007**, *304*, 640–659. [CrossRef]
34. Khorshid, E.; Alfares, M. A numerical study on the optimal geometric design of speed control humps. *Eng. Optim.* **2004**, *36*, 77–100. [CrossRef]

35. Eger, T.; Stevenson, J.; Boileau, P.É.; Salmoni, A. Predictions of health risks associated with the operation of load-haul-dump mining vehicles: Part 1—Analysis of whole-body vibration exposure using ISO 2631-1 and ISO-2631-5 standards. *Int. J. Ind. Ergon.* **2008**, *38*, 726–738. [[CrossRef](#)]
36. Kanjanavapastit, A.; Thitinaruemit, A. Estimation of a speed hump profile using quarter car model. *Procedia-Soc. Behav. Sci.* **2013**, *88*, 265–273. [[CrossRef](#)]
37. Ardeh, H.A.; Shariatpanahi, M.; Bahrami, M.N. Multiobjective shape optimization of speed humps. *Struct. Multidiscip. Optim.* **2008**, *37*, 203–214. [[CrossRef](#)]
38. Cantisani, G.; Loprencipe, G. Road roughness and whole body vibration: Evaluation tools and comfort limits. *J. Transp. Eng.* **2010**, *136*, 818–826. [[CrossRef](#)]
39. Loprencipe, G.; Pantuso, A. A specified procedure for distress identification and assessment for urban road surfaces based on PCI. *Coatings* **2017**, *7*, 65. [[CrossRef](#)]
40. Transportation Research Board. *Highway Capacity Manual 2000*; Transportation Research Board, The National Academies: Washington, DC, USA, 2000.
41. ASTM. *ASTM E867-06, Standard Terminology Relating to Vehicle-Pavement Systems*; ASTM International: West Conshohocken, PA, USA, 2012.
42. Perera, R.W.; Kohn, S.D.; Bemanian, S. Comparison of Road Profilers. *Transp. Res. Rec.* **1996**, *1536*, 117–124. [[CrossRef](#)]
43. Loprencipe, G.; Zoccali, P. Use of generated artificial road profiles in road roughness evaluation. *J. Mod. Transp.* **2017**, *25*, 24–33. [[CrossRef](#)]
44. ISO. Mechanical vibration and shock—Evaluation of human exposure to whole-body vibration—Part 1: General requirements Amendment 1. International Organization for Standardization. In *ISO 2631-1:1997/Amd 1:2010*; Swedish Standards Institute: Stockholm, Sweden, 2010.
45. Loprencipe, G.; Zoccali, P.; Cantisani, G. Effects of Vehicular Speed on the Assessment of Pavement Road Roughness. *Appl. Sci.* **2019**, *9*, 1783. [[CrossRef](#)]
46. Loprencipe, G.; Zoccali, P. Ride quality due to road surface irregularities: Comparison of different methods applied on a set of real road profiles. *Coatings* **2017**, *7*, 59. [[CrossRef](#)]
47. Ministero Delle Infrastrutture e Dei Trasporti. *Norme Funzionali e Geometriche Per La Costruzione Delle Strade*; Italian Ministry of Transportation Decreto Ministeriale: Rome, Italy, 2001.
48. Italian Parliament. *Codice Della Strada*; Italian Parliament Decreto Legislativo: Rome, Italy, 1992.
49. *Regolamento di Esecuzione e di Attuazione Del Codice Della Strada*; Decree of the President of the Italian Republic: Rome, Italy, 1992.



© 2019 by the authors. Licensee MDPI, Basel, Switzerland. This article is an open access article distributed under the terms and conditions of the Creative Commons Attribution (CC BY) license (<http://creativecommons.org/licenses/by/4.0/>).